

CDF EVIDENCE FOR THE TOP QUARK AND B PHYSICS AT FERMILAB

Weiming Yao*

Lawrence Berkeley Laboratory

Berkeley, California 94720

E-mail: weiming@fnald.fnal.gov

ABSTRACT

We present the first direct evidence for the top quark with the Collider Detector at Fermilab (CDF) in a sample of $\bar{p}p$ collisions at $\sqrt{s} = 1.8$ TeV with an integrated luminosity of 19.3 pb^{-1} . The recent B physics results at Fermilab from both collider and fixed target experiments are reviewed.

1 CDF Evidence for the Top Quark

1.1 Introduction

The Standard Model has enjoyed outstanding success, yet the top quark, which is required as the weak-isospin partner of the bottom quark, has remained unobserved. Direct searches at the Fermilab Tevatron have placed a 95% confidence level lower limit of $M_{top} > 131 \text{ GeV}/c^2$ (Ref. 2). Global fits to precision electroweak measurements yield a favored mass of $M_{top} = 177_{-11-19}^{+11+18} \text{ GeV}/c^2$ (Ref. 3).

One expects that, at Tevatron energies, most top quarks are produced in pairs. For $M_{top} \geq 85 \text{ GeV}/c^2$, each top quark decays to a real W boson and a b quark. The observed event topology is then determined by the decay mode of the two W bosons. About 5% of the time, both W bosons decay to $e\nu$ or $\mu\nu$ (the “dilepton mode”), giving two high- P_T leptons with opposite charge, two b jets, and large missing transverse energy (\cancel{E}_T) from the undetected neutrinos.⁴ In another 30% of the cases, one W boson decays to $e\nu$ or $\mu\nu$, and the other to a $q\bar{q}'$ pair (the “lepton + jets mode”). This final state includes a high- P_T charged lepton, \cancel{E}_T , and jets from the W and the two b quarks. The remaining 65% of the final states involve the hadronic decays of both W bosons, or the decay of one or both of the W bosons into τ leptons. These channels have larger backgrounds and are not considered here. This analysis is based on a sample of $\bar{p}p$ collisions at $\sqrt{s} = 1.8 \text{ TeV}$ with an integrated luminosity of $19.3 \pm 0.7 \text{ pb}^{-1}$, collected at the Fermilab Tevatron by the CDF detector⁵ in 1992–1993. The details of the analysis are presented in Ref. 1.

The momenta of charged particles are measured in the central tracking chamber (CTC), which sits inside a 1.4-T superconducting solenoidal magnet. Outside the CTC, electromagnetic and hadronic calorimeters, arranged in a projective tower geometry, cover the pseudorapidity region $|\eta| < 3.6$, allowing reliable measurements of the \cancel{E}_T . The calorimeters are also used to identify jets and electron candidates. Outside the calorimeters, drift chambers in the region $|\eta| < 1.0$ provide muon identification. A Silicon Vertex Detector (SVX),⁶ located immediately outside the beampipe, provides precise track reconstruction in the plane transverse to the beam and is used to identify secondary vertices that can be produced by b and c quark decays. A three-level trigger selects the inclusive electron and muon events used in this analysis.

1.2 Dilepton Search

In the dilepton search, both leptons are required to have $P_T > 20$ GeV/c and to have opposite charge. At least one of the leptons is required to have $|\eta| < 1.0$ and to be isolated.¹ In addition, we require $\cancel{E}_T > 25$ GeV (Ref. 7). To remove background from Z production, we reject ee and $\mu\mu$ events with $75 < M_{\ell\ell} < 105$ GeV/c². For $M_{top} > 120$ GeV/c², the two b quarks have significant energy and are detected with good efficiency as jets. By requiring two jets with $|\eta| < 2.4$ and $E_T > 10$ GeV (Ref. 7), we reduce backgrounds by a factor of four while preserving 84% of the signal for $M_{top} = 160$ GeV/c². To achieve additional rejection against $Z \rightarrow \tau\tau$ events and events with \cancel{E}_T induced by jet mismeasurement, we require, for $\cancel{E}_T < 50$ GeV, that the azimuthal angle between the \cancel{E}_T and the nearest lepton or jet exceed 20°. No ee or $\mu\mu$ events pass all cuts. Two $e\mu$ events survive.

We use the ISAJET⁸ Monte Carlo program to determine the acceptance and the efficiency of the event-selection criteria. The fractional uncertainty in the efficiency of the two-jet requirement, due mostly to the limited understanding of gluon radiation, decreases from 13% for $M_{top} = 120$ GeV/c² to 3% for $M_{top} = 180$ GeV/c². Other uncertainties in the detection efficiency come from the lepton-identification cuts (6%), lepton-isolation cuts (2%), \cancel{E}_T cuts (2%), structure functions (2%), and Monte Carlo statistics (3%). The overall acceptance, ϵ_{DIL} , for the dilepton search is shown in Table 1. The number of expected dilepton events from

M_{top}	120 GeV/c ²	140 GeV/c ²	160 GeV/c ²	180 GeV/c ²
ϵ_{DIL}	0.49 ± 0.07%	0.66 ± 0.07%	0.78 ± 0.07%	0.86 ± 0.07%
ϵ_{SVX}	1.0 ± 0.3%	1.5 ± 0.4%	1.7 ± 0.5%	1.8 ± 0.6%
ϵ_{SLT}	0.84 ± 0.17%	1.1 ± 0.2%	1.2 ± 0.2%	1.3 ± 0.2%
$\sigma_{t\bar{t}}^{Theor}$ (pb)	38.9 ^{+10.8} _{-5.2}	16.9 ^{+3.6} _{-1.8}	8.2 ^{+1.4} _{-0.8}	4.2 ^{+0.6} _{-0.4}
$\sigma_{t\bar{t}}^{Expt}$ (pb)	22.7 ^{+10.0} _{-7.9}	16.8 ^{+7.4} _{-5.9}	14.7 ^{+6.5} _{-5.1}	13.7 ^{+6.0} _{-4.7}

Table 1: Summary of top acceptance (including branching ratios) and the theoretical cross section.⁹ The last line gives the $t\bar{t}$ production cross section obtained from this measurement.

$t\bar{t}$ production, using this acceptance and the theoretical cross section,⁹ is shown in Table 2.

N_{jet}	Electrons	Muons	Total	VECBOS ($Q^2 = \langle P_T^2 \rangle$)
0 Jet	10,663	6,264	16,927	—
1 Jet	1058	655	1713	1571^{+285}_{-227}
2 Jets	191	90	281	267^{+80}_{-57}
3 Jets	30	13	43	39^{+12}_{-10}
≥ 4 Jets	7	2	9	$7^{+3.2}_{-2.2}$

Table 2: Summary of W candidate event yields as a function of jet multiplicity. Jets have $E_T \geq 15$ GeV and $|\eta| \leq 2.0$. Also shown are the predicted number of W events from the VECBOS Monte Carlo program. The uncertainties shown in the VECBOS predictions are dominated by the uncertainty in the jet energy scale; the uncertainty in the Q^2 scale is not included.

The dilepton background from WW production is calculated using ISAJET, assuming a total WW cross section of 9.5 pb (Ref. 10), and is found to be 0.16 ± 0.06 events. WW events may contain two jets due to initial-state gluon radiation. The treatment of initial-state radiation in the ISAJET calculation is checked using $Z + jets$ data, and good agreement is found. The background from $Z \rightarrow \tau\tau$ is estimated using $Z \rightarrow ee$ data, where each electron is replaced by a simulated τ that decays leptonically. This background contributes 0.13 ± 0.04 events. We estimate backgrounds from $b\bar{b}$ and $c\bar{c}$ using ISAJET to model production processes, and the CLEO Monte Carlo program¹¹ to model B -meson decay. The Monte Carlo rates are normalized to a sample of $e\mu$ data collected with lower trigger thresholds. We estimate 0.10 ± 0.06 background events from these sources. Backgrounds from hadrons misidentified as leptons (0.07 ± 0.05 events) and the Drell-Yan production of lepton pairs ($0.10^{+0.23}_{-0.08}$) are estimated from inclusive-jet and Z data, respectively. The total expected background is $0.56^{+0.25}_{-0.13}$ events, with two candidates observed.

1.3 Lepton-Plus-Jets Search

Events selected for the lepton + jets search are required to have an isolated lepton with E_T (P_T for muons) > 20 GeV and $|\eta| < 1.0$, and to have $\cancel{E}_T > 20$ GeV (Ref. 7). Events containing Z bosons are removed by rejecting events with an ee or $\mu\mu$ invariant mass between 70 and 110 GeV/ c^2 . In Table 2, we classify the remaining events according to the multiplicity, N_{jet} , of jets with $E_T > 15$ GeV and $|\eta| < 2.0$ (Ref. 7).

The dominant background in the lepton + jets search is the direct production of W + jets. The ratio of the $t\bar{t}$ signal to W + jets background can be greatly improved by requiring $N_{jet} \geq 3$. This requirement has a rejection factor of ≈ 400 against inclusive W production while keeping approximately 75% of the $t\bar{t}$ signal in the lepton + jets mode for $M_{top} = 160$ GeV/ c^2 . In the W + ≥ 3 -jet sample, we expect 12 ± 2 (6.6 ± 0.7) $t\bar{t}$ events for $M_{top} = 160$ (180) GeV/ c^2 , using the acceptance discussed below and the theoretical cross section. We observe 52 events with $N_{jet} \geq 3$.

The VECBOS Monte Carlo program¹² can be used to make estimates of direct W + jets production. Table 3 shows the results of a particular calculation which predicts 46 events with ≥ 3 jets and seven events with ≥ 4 jets. The VECBOS predictions for ≥ 3 jets have uncertainties of about a factor of two due to the choice of Q^2 scale and cannot be used for a reliable absolute background calculation. We therefore have developed a technique for estimating backgrounds in the lepton + jets search directly from the data. This technique is described below. Other backgrounds (direct $b\bar{b}$, Z bosons, W pairs, and hadrons misidentified as leptons) contribute 12.2 ± 3.1 events.¹ Additional background rejection is needed to isolate a possible $t\bar{t}$ signal. Requiring the presence of a b quark, tagged either by a secondary vertex or by a semileptonic decay, provides such rejection.

1.3.1 SVX b-Tag

The lifetime of b hadrons can cause the b -decay vertex to be measurably displaced from the $\bar{p}p$ interaction vertex. When associated with jets with $E_T > 15$ GeV and $|\eta| < 2.0$, SVX tracks with $P_T \geq 2$ GeV/ c and impact-parameter significance $|d|/\sigma_d \geq 3$ are used in a vertex-finding algorithm.¹ Using these tracks, the decay length transverse to the beam, L_{xy} , and its uncertainty (typically $\sigma_{L_{xy}} \approx 130$ μm) are calculated using a three-dimensional fit, with the tracks constrained to origi-

nate from a common vertex. Jets that have a secondary vertex displaced in the direction of the jet, with significance $|L_{xy}|/\sigma_{L_{xy}} \geq 3.0$, are defined to be ‘‘SVX-tagged.’’

We use a control sample, enriched in b -decays, of inclusive electrons ($E_T > 10$ GeV) to measure the efficiency for SVX-tagging a semileptonic b jet.¹ We compare this efficiency with that predicted by the ISAJET + CLEO $b\bar{b}$ Monte Carlo and find our measured efficiency to be lower than the Monte Carlo prediction by a factor of 0.72 ± 0.21 . We then determine the efficiency for tagging at least one b jet in a $t\bar{t}$ event with three or more observed jets, ϵ_{tag} , from $t\bar{t}$ Monte Carlo rescaled by the factor determined above. We find $\epsilon_{tag} = 22 \pm 6\%$ independent of top mass for $M_{top} > 120$ GeV/ c^2 . The efficiency, ϵ_{SVX} , for inclusive $t\bar{t}$ events to pass the lepton-identification, kinematic, and SVX b -tag requirements is shown in Table 1. The number of expected SVX-tagged $t\bar{t}$ events with $N_{jet} \geq 3$ is shown in Table 2. Six SVX-tagged events are observed in the 52-event $W + \geq 3$ -jet sample.

Rather than rely on Monte Carlo predictions, we estimate directly from our data how many tags we would expect in the 52-event sample if it were entirely background. We assume that the heavy-quark (b and c) content of jets in $W +$ jets background events is the same as in an inclusive-jet sample.¹ This assumption is expected to be conservative, since the inclusive-jet sample contains heavy-quark contributions from direct production (e.g., $gg \rightarrow b\bar{b}$), gluon splitting (where a final-state gluon branches into a heavy-quark pair), and flavor excitation (where an initial-state gluon excites a heavy quark in the proton or antiproton sea), while heavy quarks in $W +$ jets background events are expected to be produced almost entirely from gluon splitting.¹³ We apply the tag rates measured in the inclusive-jet sample, parametrized by the E_T and track multiplicity of each jet, to the jets in the 52 events to yield the total expected number of SVX-tagged events from $Wb\bar{b}$, $Wc\bar{c}$, and fake tags due to track mismeasurement. We have tested this technique in a number of control samples and use the level of agreement with the number of observed tags to determine the systematic uncertainty on the predicted tag rate. The backgrounds from non- W sources (direct $b\bar{b}$ production and hadrons misidentified as leptons) are also determined from the data.¹ The small contributions from Wc , from WW and WZ production, and from $Z \rightarrow \tau\tau$ are estimated from Monte Carlo events. The total estimated background to SVX tags in the 52-event sample is 2.3 ± 0.3 events. An alternate background estimate,

using Monte Carlo calculations of the heavy-quark processes in $W + \text{jets}$ events and a fake-tag estimate from jet data, predicts a heavy-quark content per jet approximately a factor of three lower than in inclusive-jet events and gives an overall background estimate of a factor of 1.6 lower than the number presented above, supporting the conservative nature of our background estimate.

In the $W + \text{jets}$ sample, the L_{xy} distribution of observed SVX tags is consistent with that of heavy-quark jets. The tags in the W events with one and two jets are expected to come mainly from sources other than $t\bar{t}$ decay, and the rate of these tags is consistent with the background prediction, with 16 events tagged and 22.1 ± 4.0 predicted.

1.3.2 SLT b-Tag

A second technique for tagging b quarks is to search for leptons arising from the decays $b \rightarrow \ell\nu X$ ($\ell = e$ or μ), or $b \rightarrow c \rightarrow \ell\nu X$. Because these leptons typically have lower P_T than leptons from W decays, we refer to them as “soft lepton tags,” or SLT. We require lepton $P_T > 2$ GeV/c. To keep this analysis statistically independent of the dilepton search, leptons that pass the dilepton requirements are not considered as SLT candidates.

In searching for electrons from b and c decays, each CTC track is extrapolated to the calorimeter, and a match is sought to an electromagnetic cluster consistent in size, shape, and position with expectations for electron showers. The efficiency of the electron selection criteria, excluding isolation cuts, is determined from a sample of electron pairs from photon conversions, where the first electron is identified in the calorimeter and the second, unbiased electron is selected using a track-pairing algorithm. The electron isolation efficiency is determined from $t\bar{t}$ Monte Carlo events. The total efficiencies are $(53 \pm 3)\%$ and $(23 \pm 3)\%$ (statistical uncertainties only) for electrons from b and sequential c decays, respectively. To identify muons, track segments in the muon chambers are matched to tracks in the CTC. The efficiency for reconstructing track segments in the muon chambers is measured to be 96% using $J/\psi \rightarrow \mu^+\mu^-$ and $Z \rightarrow \mu^+\mu^-$ decays. This number is combined with the P_T -dependent efficiency of the track-matching requirements to give an overall efficiency of approximately 85% for muons from both b and c decays.

The acceptance of the SLT analysis for $t\bar{t}$ events is calculated using the ISAJET and CLEO Monte Carlo programs. The efficiency for tagging at least one jet in a $t\bar{t}$ event by detecting an additional lepton with $P_T > 2$ GeV/c is $\epsilon_{tag} = 16 \pm 2\%$, approximately independent of M_{top} . The efficiency, ϵ_{SLT} , for inclusive $t\bar{t}$ events to pass the lepton-identification, kinematic, and SLT b -tag requirements is shown in Table 1. The number of expected SLT-tagged $t\bar{t}$ events is shown in Table 2. We find seven SLT-tagged events with $N_{jet} \geq 3$. Three of the seven also have SVX tags.

The main backgrounds to the SLT search are hadrons misidentified as leptons, and $Wb\bar{b}$, $Wc\bar{c}$ production. As in the SVX analysis, we estimate these backgrounds from the data by conservatively assuming that the heavy-quark content per jet in $W + \text{jets}$ events is the same as in inclusive-jet events. By studying tracks in such events, we measure the probability of misidentifying a hadron as an electron or muon, or of tagging a true semileptonic decay. We use these probabilities to predict the number of tags in a variety of control samples and obtain good agreement with the number observed. We expect 2.70 ± 0.27 tags in the $W + \geq 3$ -jet sample from these sources. Other sources (direct $b\bar{b}$, W/Z pairs, $Z \rightarrow \tau\tau$, Wc , and Drell-Yan) contribute 0.36 ± 0.09 events, for a total SLT background of 3.1 ± 0.3 events. The number of SLT tags in the $W + 1$ and $W + 2$ -jet samples, which should have only a small contribution from $t\bar{t}$, agrees with the background expectation (45 events tagged, 44 ± 3.4 predicted). Figure 1 shows the combined number of SVX and SLT tags, together with the estimated background, as a function of jet multiplicity.

1.4 Statistical Significance and Cross Section

Each of the analyses presented above shows an excess of events over expected backgrounds, as shown in Table 3. The dilepton analysis observes two events with a background of $0.56^{+0.25}_{-0.13}$. The lepton + jets b -tag analysis identifies ten events: six events with a background of 2.3 ± 0.3 using the SVX tagging algorithm, and seven events with a background of 3.1 ± 0.3 using the SLT tagging algorithm, with three of these events tagged by both algorithms.

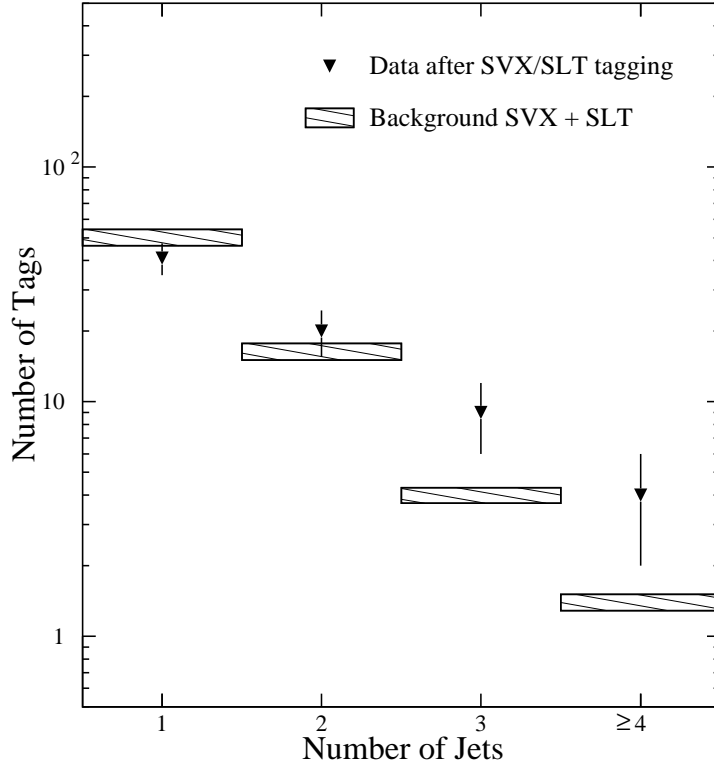


Figure 1: The sum of SVX and SLT tags observed in the W + jets data (solid triangles). Events tagged by both algorithms are counted twice. The shaded area is the sum of the background estimates for SVX and SLT, with its uncertainty. The three-jet and four-or-more-jet bins are the $t\bar{t}$ signal region.

Channel	Dilepton	SVX	SLT
$N_{expected}, M_{top} = 120 \text{ GeV}/c^2$	3.7 ± 0.6	7.7 ± 2.5	6.3 ± 1.3
$N_{expected}, M_{top} = 140 \text{ GeV}/c^2$	2.2 ± 0.2	4.8 ± 1.7	3.5 ± 0.7
$N_{expected}, M_{top} = 160 \text{ GeV}/c^2$	1.3 ± 0.1	2.7 ± 0.9	1.9 ± 0.3
$N_{expected}, M_{top} = 180 \text{ GeV}/c^2$	0.68 ± 0.06	1.4 ± 0.4	1.1 ± 0.2
Total Background	$0.56^{+0.25}_{-0.13}$	2.3 ± 0.3	3.1 ± 0.3
Observed Events	2	6	7

Table 3: Number of $t\bar{t}$ events expected assuming the theoretical cross section, and the number of candidate events observed with expected backgrounds.

For each of these results, we calculate the probability, \mathcal{P} , that the estimated background has fluctuated up to the number of candidate events seen or greater. We find $\mathcal{P}_{DIL} = 12\%$, $\mathcal{P}_{SVX} = 3.2\%$, and $\mathcal{P}_{SLT} = 4.1\%$.

To calculate the probability $\mathcal{P}_{combined}$ that all three results together are due only to an upward fluctuation of the background, we use the observation of 15 “counts”: the two dilepton events, the six SVX tags, and the seven SLT tags. This procedure gives extra weight to the double-tagged events, which are approximately six times more likely to come from b and c jets than from fakes, and therefore have a significantly smaller background than the single-tagged events. We have checked that we understand SVX–SLT correlations by correctly predicting the number of double-tagged jets and events in the inclusive-jet sample. We calculate $\mathcal{P}_{combined}$ using a Monte Carlo program that generates many samples of 52 background events, with fractions of W + light quark and gluon jets, $Wb\bar{b}$, $Wc\bar{c}$, and other backgrounds distributed according to Poisson statistics with mean values and uncertainties predicted by Monte Carlo calculations.¹ The number of events with heavy-quark jets is scaled up to agree with the more conservative background estimate from inclusive-jet data. The predicted number of SVX plus SLT-tagged events is obtained by applying the measured efficiencies and correlations in the SVX and SLT fake rates. This number is combined with a Poisson-distributed number of dilepton background events to determine the fraction of experiments with 15 or more counts from background alone. We find $\mathcal{P}_{combined} = 0.26\%$. This corresponds to a 2.8σ excess for a Gaussian probability function.

Assuming the excess events to be from $t\bar{t}$, we calculate the cross section for $t\bar{t}$ production in $p\bar{p}$ collisions at $\sqrt{s} = 1.8$ TeV. The calculation uses the $t\bar{t}$ acceptance, the derived efficiencies for tagging jets in $t\bar{t}$ events, and a revised estimate of the background appropriate for a mixture of $t\bar{t}$ events and background in the 52-event W + jets sample (rather than assuming it to contain all background as above). In Table 1, we summarize the acceptances, and the theoretical and measured cross sections as a function of M_{top} .

1.5 Top Mass Measurement

Assuming that the excess of b -tagged events is due to $t\bar{t}$ production, we estimate M_{top} using a constrained fit¹⁴ to each tagged event with four jets. Using the 52-event $W + \geq 3$ -jet sample, we require a fourth jet with $E_T > 8$ GeV and

$|\eta| < 2.4$. Seven of the ten b -tagged events identified in the lepton + jets analysis pass this requirement. These seven events are fitted individually to the hypothesis that three of the jets come from one t or \bar{t} through its decay to Wb , and that the lepton, \cancel{E}_T , and the remaining jet come from the other t or \bar{t} decay.⁷ If the event contains additional jets, only the four highest- E_T jets are used in the fit. The fit is made for all six jet configurations, with the requirement that the tagged jet in the event must be one of the b quarks. There are two solutions in each case for the longitudinal momentum of the neutrino, and the one corresponding to the best χ^2 is chosen.

Application of this method to $t\bar{t}$ Monte Carlo events ($M_{top} = 170 \text{ GeV}/c^2$) gives a distribution with a peak at $168 \text{ GeV}/c^2$ and a rms spread of $23 \text{ GeV}/c^2$. Fitting Monte Carlo W + jets background events to the $t\bar{t}$ hypothesis yields a mass distribution with a broad peak centered at about $140 \text{ GeV}/c^2$.

The results of the fits to the seven events are presented in Fig. 2. In this sample, $1.4_{-1.1}^{+2.0}$ events are expected to come from background.¹

To find the most likely top mass from the seven events, we perform a likelihood fit of their mass distribution to a sum of the expected distributions from W + jets and a top quark of mass M_{top} . The $-\log(\text{likelihood})$ distribution from this fit is shown in the inset to Fig. 2. Systematic uncertainties in this fit arise from the background estimation, the effects of gluon radiation on the determination of parton energies, the jet energy scale, kinematic bias in the tagging algorithms, and different methods of performing the likelihood fit. Combining these uncertainties yields a top mass of $M_{top} = 174 \pm 10_{-12}^{+13} \text{ GeV}/c^2$, where the first uncertainty is statistical and the second is systematic. The statistical uncertainty includes the effects of detector resolution and incorrect assignments of jets to their parent partons. Using the acceptance for this top mass and our measured excess over background, we find $\sigma_{t\bar{t}}(M_{top} = 174 \text{ GeV}/c^2) = 13.9_{-4.8}^{+6.1} \text{ pb}$. By performing a simple χ^2 analysis on the theoretical prediction for the cross section as a function of M_{top} , our measured mass, and our measured cross section, we find that the three results are compatible at a confidence level of 13% (1.5σ).

1.6 Conclusions and Prospects for Run 1B

We have performed many consistency checks, and have found some features of the data that do not support the $t\bar{t}$ hypothesis. The sample of inclusive Z events

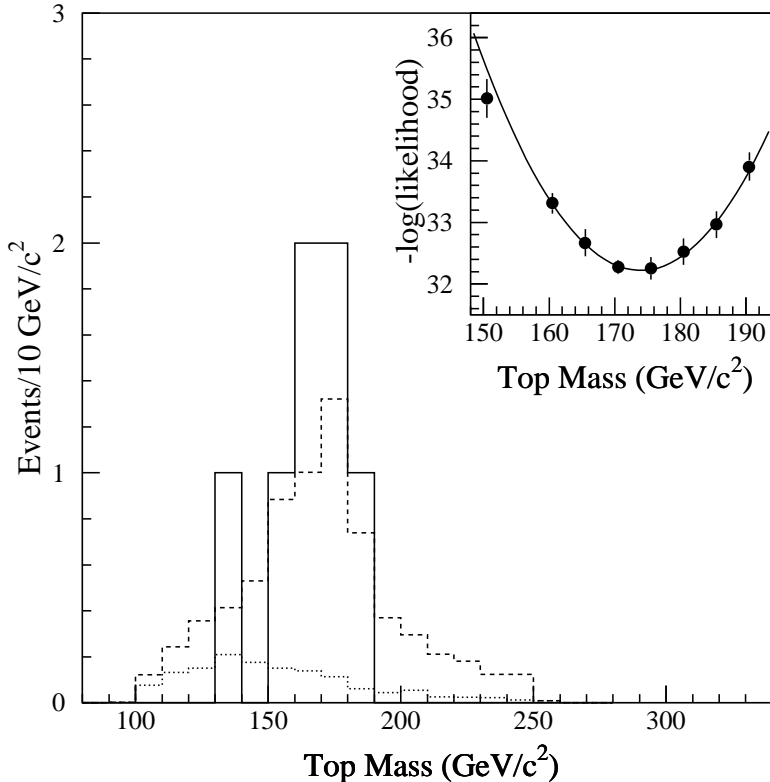


Figure 2: Top mass distribution for the data (solid histogram), the $W + \text{jets}$ background (dots), and the sum of background + Monte Carlo $t\bar{t}$ for $M_{top} = 175 \text{ GeV}/c^2$ (dashed). The background distribution has been normalized to the 1.4 background events expected in the mass-fit sample. The inset shows the likelihood fit used to determine the top mass.

serves as a control sample for studying the production of a vector boson plus jets, as Z bosons are not produced in $t\bar{t}$ decay. We find two b -tagged $Z + \geq 3$ -jet events with 0.64 expected. Both events have four jets and are SVX-tagged. Though the statistics are limited, these events could indicate an additional (non- $t\bar{t}$) source of vector boson plus heavy quark production, not accounted for in our background estimates. Higher-statistics checks of the b -tagging rate in W or $Z + 1$ and 2-jet events are consistent with expectations. We also find that the measured $t\bar{t}$ cross section is large enough to account for all observed $W + 4$ -jet events. The apparent deficit of events from direct production of $W + 4$ jets and other backgrounds is a 1.5 – 2σ effect.

Other features do support the $t\bar{t}$ hypothesis. One of the dilepton candidate events is b -tagged by both the SVX and SLT algorithms, with approximately 0.01

double-tagged background events (0.13 signal events) expected. This, together with the excess of b -tagged $W + \text{jets}$ events, provides evidence for an excess of both $Wb\bar{b}$ and $WWb\bar{b}$ production, as expected from $t\bar{t}$ decays. We have performed a kinematic analysis of the lepton + jets sample and conclude that it can accommodate the top content implied by our measured cross section. Furthermore, a likelihood fit to the top mass distributions obtained from the b -tagged $W + 4\text{-jet}$ events prefers the $t\bar{t} + \text{background}$ hypothesis over the background-only hypothesis by 2.3 standard deviations.

In conclusion, the data presented here give evidence for, but do not firmly establish, the existence of the top quark. Work is continuing on kinematic analyses of the present data, and we hope for an approximate four-fold increase in data from the 1994-95 Tevatron collider run.

2 B Physics at Fermilab

2.1 Introduction

The advantages of studying B physics at Tevatron include the relatively large cross-section for b -quark production and the broad range of B hadrons which are produced, including B_u , B_d , B_s , B_c , and Λ_b . This is different than the situation in e^+e^- machines that make use of either $\Upsilon(4S)$ in which only the light B mesons produced, or $Z \rightarrow b\bar{b}$ at LEP in which the production rate is many orders of magnitude smaller than at the Tevatron. Furthermore, with the high resolution SVX and generalized triggers, such as dilepton and single-lepton triggers, it makes Tevatron a unique place to have a broad B-physics program. Figure 3 illustrates the CDF B physics capability showing a top decay where both b 's decay vertices are clearly detected by SVX.

2.2 b Cross Section

2.2.1 Fixed-Target b Production

Due to heavy b -quark mass, fixed-target b production can be understood in terms of the predictions of perturbative QCD. Consequently, the measurement of b -quark production using fixed-target experiments provides an opportunity to test QCD. The current b cross-section measurements are in good agreement with NLO

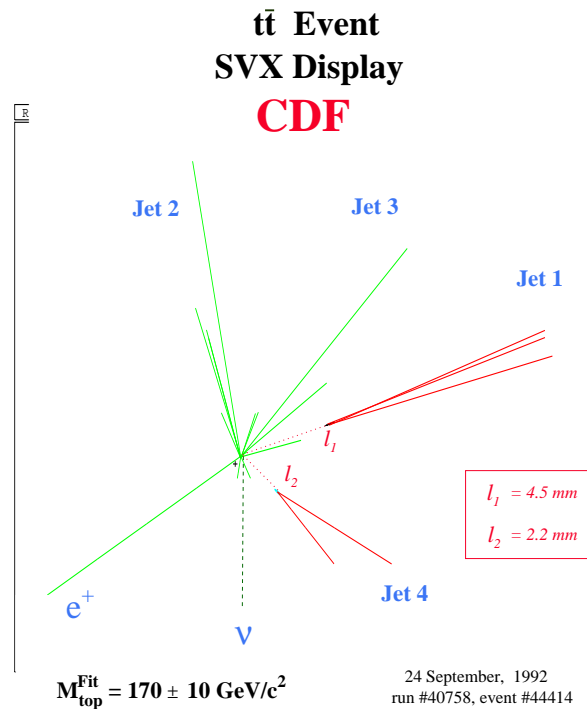


Figure 3: The top event has two secondary vertices identified by the CDF Silicon Vertex Detector.

QCD calculations, but are still statistics limited. E-672/702 at Fermilab detected a sample of J/ψ mesons coming from secondary vertices during the 1990 Fermilab fixed-target run with a $520 \text{ GeV}/c \pi^-$ beam incident on beryllium and copper targets.¹⁵ Based upon ten events coming from a secondary vertex occurring in an air-gap between their targets, they found an inclusive $b\bar{b}$ cross section of $75 \pm 28 \pm 23 \text{ nb/nucleon}$, which is in good agreement with recent QCD predictions. Similarly, E-789 at Fermilab has also measured the b cross section by comparing the number of upstream and downstream J/ψ 's detected in their limited acceptance mass focusing spectrometer.¹⁶ Their result is also in good agreement with QCD prediction.

2.2.2 Collider b Production

Measurements of the b production cross section at the Tevatron collider provide an interesting testing ground for next-leading-order QCD calculations. Studying the B meson spectra provides important engineering numbers for predicting the

sensitivity of further experiments toward measuring CP violation parameters. In the past, heavy quark production cross sections were determined using inclusive lepton or charmonium (ψ and ψ') data samples from CDF. Inclusive lepton cross sections¹⁷ allow a high statistics measurement of the b cross section at Tevatron. The systematic uncertainties in these measurements are dominated by the level of understanding for the background. The inclusive ψ and ψ' channels¹⁸ provide a clean signature of heavy quark decay and can be easily separated from background due to excellent mass resolution, but converting a charmonium cross section to a b cross section requires knowledge of the fraction of these ψ states that come from b decays. The momentum of the b quarks were also not well-known in both cases and had to be determined from the daughter's momentum, which made the results model dependent. With the CDF SVX and large data samples, these problems have been greatly reduced by studying fully reconstructed exclusive or semiexclusive final states. For example, Fig. 4 shows the size of $B \rightarrow \psi K$ mass peak from the CDF experiment as well as $B \rightarrow lD^{*\pm}X$ with the fully reconstructed $D^{*\pm}$ through $D^{*\pm} \rightarrow D^0\pi^\pm$ and $D^0 \rightarrow K\pi$.

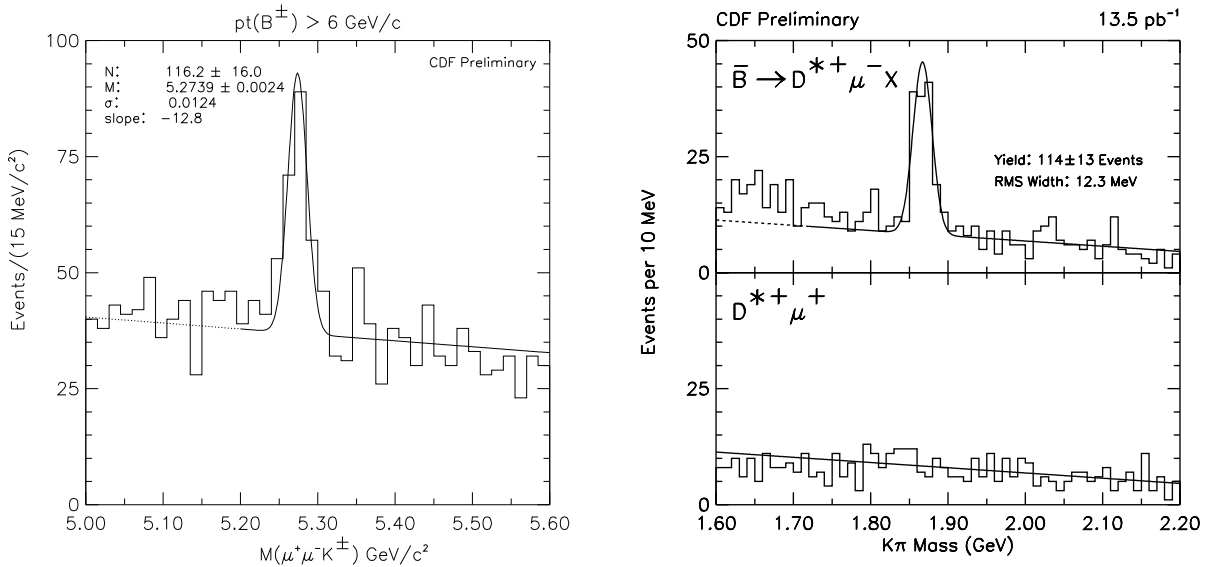


Figure 4: (a) The invariant mass distribution of $J/\psi + K^\pm$ in run 1A data. The invariant mass distribution of $K\pi$ in (b) right-sign combination (clear signal) and (c) wrong-sign combination (no signal).

A summary of the CDF b cross-section measurements is shown in Fig. 5, which appears to be a factor of two above the QCD predictions. CDF also measured the differential cross section for B-meson production using its exclusive decay modes shown in Fig. 5. Again, the measured cross section is about a factor of two higher than theory.

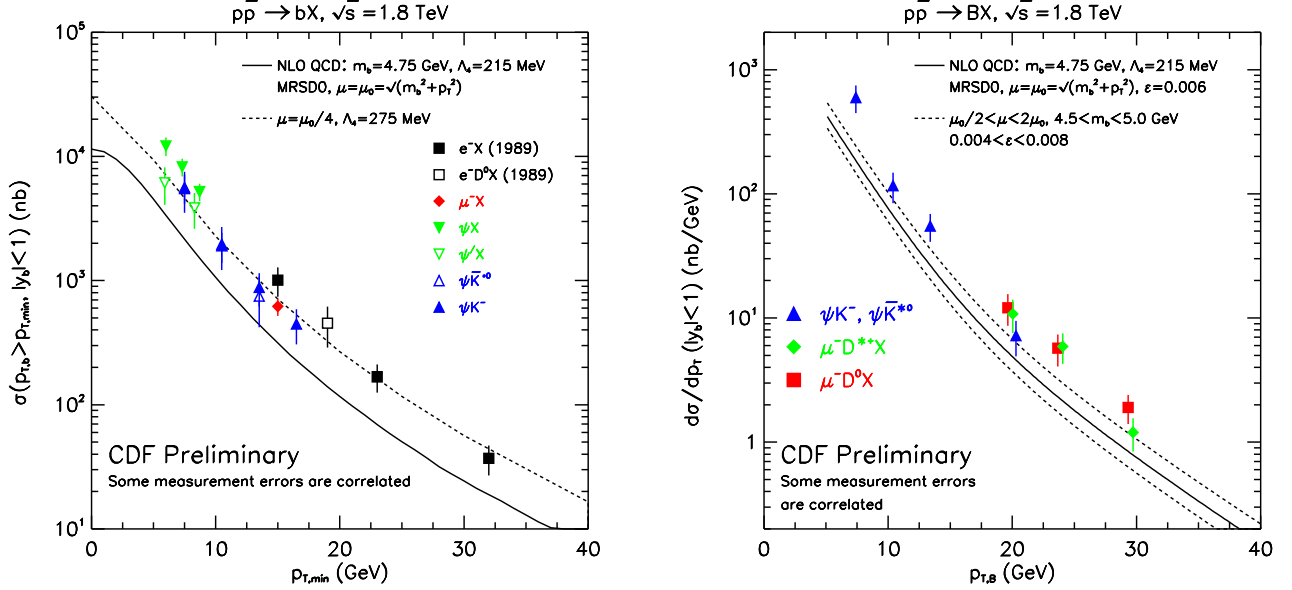


Figure 5: (a) CDF b -production cross section. (b) B-meson differential cross section from CDF compared to a next-leading-order QCD calculation.

Similarly, DØ has measured the b cross section using inclusive single-muon and dimuon samples.¹⁹ The DØ inclusive b cross section from inclusive muon samples is shown in Fig. 6, which appears to be in good agreement with NLO QCD predictions. It is noted that the theoretical curves are used differently by CDF and DØ. Within the quoted uncertainties, the two data sets are in good agreement.

2.3 b Lifetime Measurements

In this section, we report on two B-lifetime measurements at CDF using fully²⁰ and semiexclusive reconstructed decays.²¹ The data sample used in these analyses is based on 19.3 pb^{-1} data collected at CDF during the 1992–1993 period. The

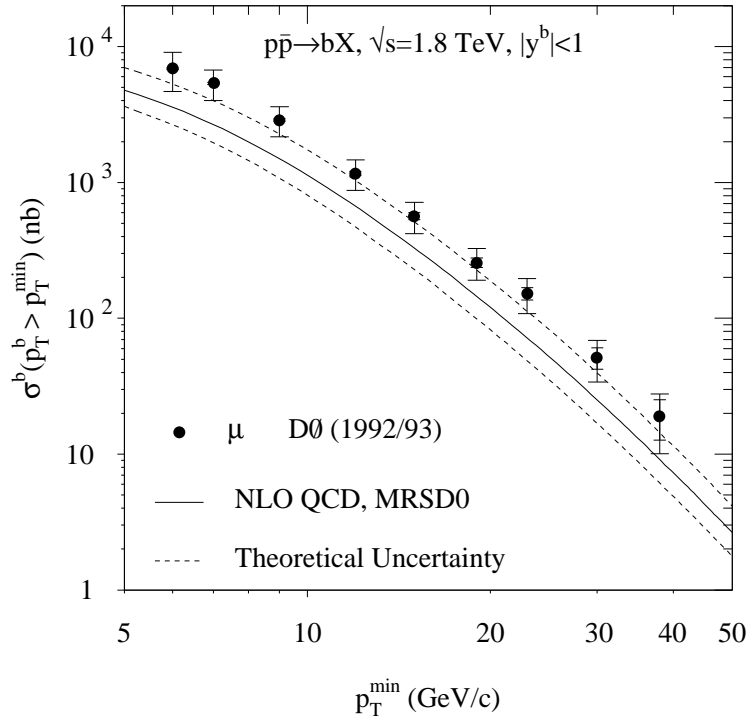


Figure 6: The D0 b -production cross-section measurement using an inclusive muon sample.

B-meson lifetime is sensitive to the details of the decay mechanism beyond the spectator model. The B-decay model predicts a very small difference between charged and neutral B-meson lifetimes of about 5%. This difference is not true in the charm meson case. Reaching this precision would provide a direct test of the validity of the B-decay model.

2.3.1 Exclusive B_u and B_d Lifetime

In this case where the B meson is fully reconstructed, the B-meson type, $\beta\gamma$, and decay length are all precisely determined. It has small systematic uncertainties but is statistically limited by the number of fully reconstructed B mesons. In order to increase the sample size, all possible decay modes $B \rightarrow \psi \mathbf{K}$ have been used, where ψ represents J/ψ and $\psi(2s)$. \mathbf{K} represents the different kaon states including K^\pm , $K^{*\pm}$, K_s^- , and K^{*0} . In addition, both muons are required to have

SVX information in order to have an adequate secondary vertex resolution. All the decay tracks, except from a K_s decay, are vertex constrained and the J/ψ and $\psi(2s)$ candidates are mass constrained to their known masses.²² Any B's with $P_T(B) < 6.0 \text{ GeV}/c^2$ are rejected. In the case of multiple candidates, the one with the best χ^2 from the constrained fit is kept. The mass distribution for these candidates with and without the requirement $c\tau > 100 \mu\text{m}$ are shown in Fig. 7.

Figure 7: (a) The charged and (b) neutral B-meson invariant mass distribution.

For the lifetime analysis, the signal region is defined to be $\pm 30 \text{ MeV}$ of the world average B-meson mass. Side-band regions are defined to be between 60 MeV and 120 MeV away from the B mass, which excludes the region where B's with a missing π would be reconstructed. The decay length distribution for charged and neutral B's for both signal and sidebands are shown in Fig. 8.

The superimposed curves are the results of separate unbinned likelihood fits for charged and neutral B mesons. The preliminary measurements of the lifetime of the B^+ and B^0 mesons are shown in Table 4. The systematic errors are dominated by the residual misalignments, trigger bias, and beam stability. Work is ongoing to further increase both the statistics and the signal-to-noise ratio of B-meson reconstruction.

Figure 8: Signal and background $c\tau$ distributions for (a) charged B^\pm meson and (b) neutral B^0 meson.

2.3.2 Semileptonic B_u and B_d Lifetimes

The exclusive B lifetime measurements are limited by statistics. One way to improve the measurement is to use semileptonic B-decay modes. From an inclusive lepton sample, we search for charm mesons from $B \rightarrow lDX$ decay in a cone around

Modes	$\tau(B_u^+)$ psec	$\tau(B_d^0)$ psec	τ^+/τ^0
Full Reconstruction	$1.61 \pm 0.16 \pm 0.05$	$1.57 \pm 0.18 \pm 0.08$	$1.02 \pm 0.16 \pm 0.05$
Lepton + Charm	$1.63 \pm 0.20 \pm 0.16$	$1.62 \pm 0.16 \pm 0.15$	$1.01 \pm 0.23 \pm 0.17$

Table 4: B_u^+ , B_d^0 lifetimes and their ratios.

the lepton. The events can be divided into the following three classes:

- $D^{*-} \rightarrow D^0\pi^-$ are dominantly from B^0 decay,
- D^0 , not from D^{*-} decays, are dominantly from B^- decay,
- D^- are dominantly from B^0 decay since the D^{*0} does decay to D^- ,

where the D^0 is reconstructed through $K^-\pi^+$ mode. The sign of lepton is corrected with the sign of kaon if the lepton and D originate from the decay of a B meson. A clean D signal is seen in the invariant mass distribution of the right-sign combinations, as shown in Fig. 4, while no signal is observed in the wrong-sign combinations. The B secondary vertex is determined by intersecting the D meson and lepton. Since the neutrino is missing, the $\beta\gamma$ correction cannot be calculated directly. It is possible to estimate the boost of the B using the boost of lepton and charm and Monte Carlo. There are complications in separating charged and neutral B's due to the existence of D^{**} and due to some inefficiency in the association of the π to the D^0 to form a $D^{*\pm}$. These complications have been modeled with Monte Carlo. A combined lifetime fit yields the charged and neutral B lifetime given in Table 4. The largest systematic errors arise from the background shape, residual misalignment, the $\beta\gamma$ correction, and the D^{**} sample modeling. The CDF for the exclusive and semiexclusive analyses are both consistent and competitive with the results from LEP experiments. The comparison of the lifetime ratio of the charged to neutral B meson is shown in Fig. 9.

2.3.3 B_s Lifetime

A similar technique has been applied to measure B_s meson lifetimes using both the exclusive decay to $J/\psi\phi$ and the semileptonic $B_s \rightarrow l\nu D_s$, $D_s \rightarrow \phi\pi$, $\phi \rightarrow K^+K^-$ decays.²³ In the exclusive case (Fig. 10), the result is limited by statistics: $\tau_{B_s} = 1.74_{-0.69}^{+1.08} \pm 0.07$ psec. In the semileptonic case, there are about 76 D_s candidates found in the combined inclusive electron and muon samples. Figure 10(b) shows the invariant mass of the $K^+K^-\pi$ system. A clean signal of D_s is seen in the right-sign combination while no signal is observed in the wrong-sign combination. A combined fit to lifetime distributions of signal and background

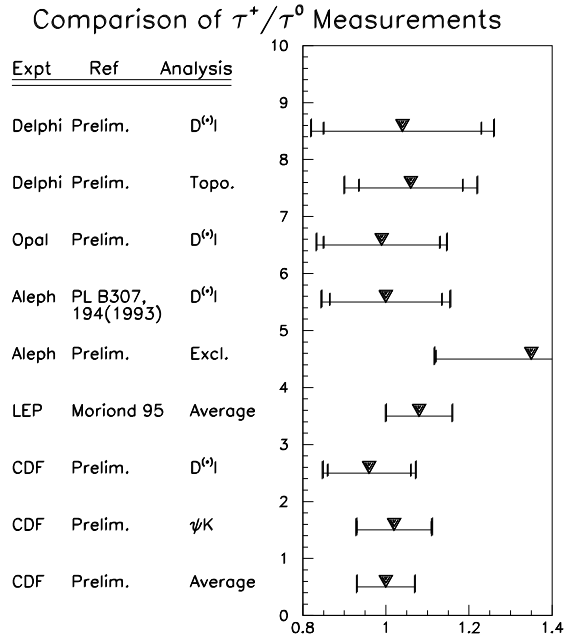


Figure 9: The comparison of the lifetime ratio of the charged to neutral B mesons (updated to March 1995).

yields the $\tau_{B_s} = 1.42_{-0.23}^{+0.27} \pm 0.11$ psec. The result is limited by statistics. We expect to improve the measurement in the near future by adding run 1B data.

2.4 Polarization Measurement of $B \rightarrow J/\psi K^*$

We report on a measurement of the polarization in the decay $B^0 \rightarrow J/\psi K^{*0}$ using 19.3 pb^{-1} data collected at CDF.²⁴ The pseudoscalar to vector-vector decay $B^0 \rightarrow J/\psi K^{*0}$ allows different polarizations in the final state. The measurement of this polarization tests the factorization hypothesis for hadronic decays and also helps determine if the decay is useful for studies of CP violation. B^0 mesons were reconstructed through the decay chain $B^0 \rightarrow J/\psi K^{*0}$, $J/\psi \rightarrow \mu^+ \mu^-$, and $K^{*0} \rightarrow K^+ \pi^-$. The polarization was determined using the measured helicity angles θ_{K^*} and θ_ψ , where θ_{K^*} is the decay angle of the kaon in the K^{*0} rest frame with respect to the K^{*0} direction in the B^0 rest frame, and θ_ψ is the decay angle of the muon in the J/ψ rest frame with respect to the J/ψ direction in the B^0

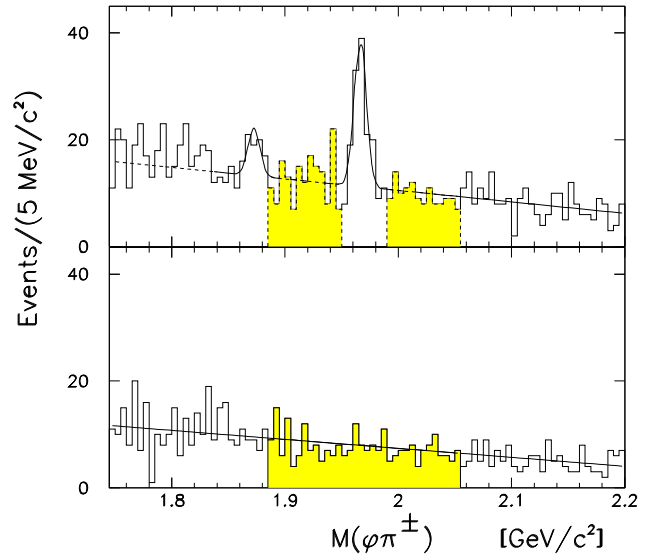
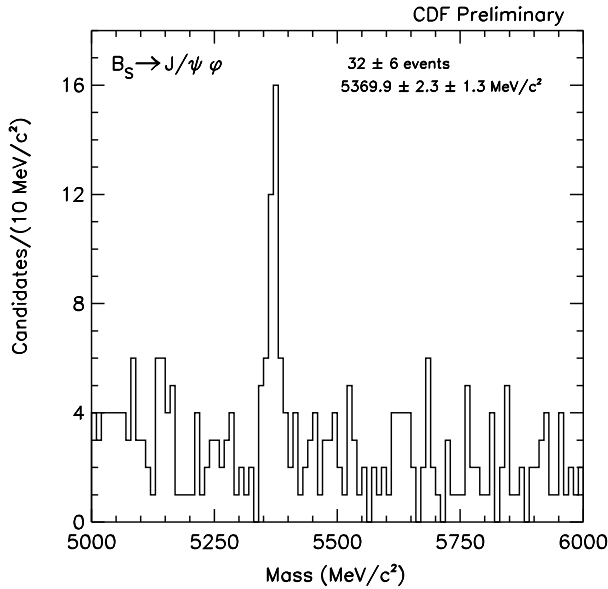


Figure 10: (a) The $B_s \rightarrow J/\psi\phi$ mass peak at CDF. (b) The $D_s \rightarrow \phi\pi$ and $\phi \rightarrow K^+K^-$ invariant mass distribution—the upper plot is the right sign, and the bottom plot is the wrong sign.

rest frame. An unbinned likelihood fit results in a polarization measurement of $\Gamma_L/\Gamma = 0.66 \pm 0.10(stat)_{-0.10}^{+0.08}(sys)$, which is in good agreement with the recent CLEO measurement.²⁵ The superimposed curves shown in Fig. 11 are the results of the unbinned likelihood fits after background and acceptance correction. The systematic error is dominated by the uncertainty associated with the background estimation.

2.5 Conclusion and Prospects for Run 1B

With the run 1A data, CDF has improved the understanding of b production, produced competitive lifetime results, and started to search for new particles and rare decays. Run 1B has started, and we expect to accumulate another 100 pb^{-1} of data. With trigger improvements, updated DAQ, and a new radiation hard

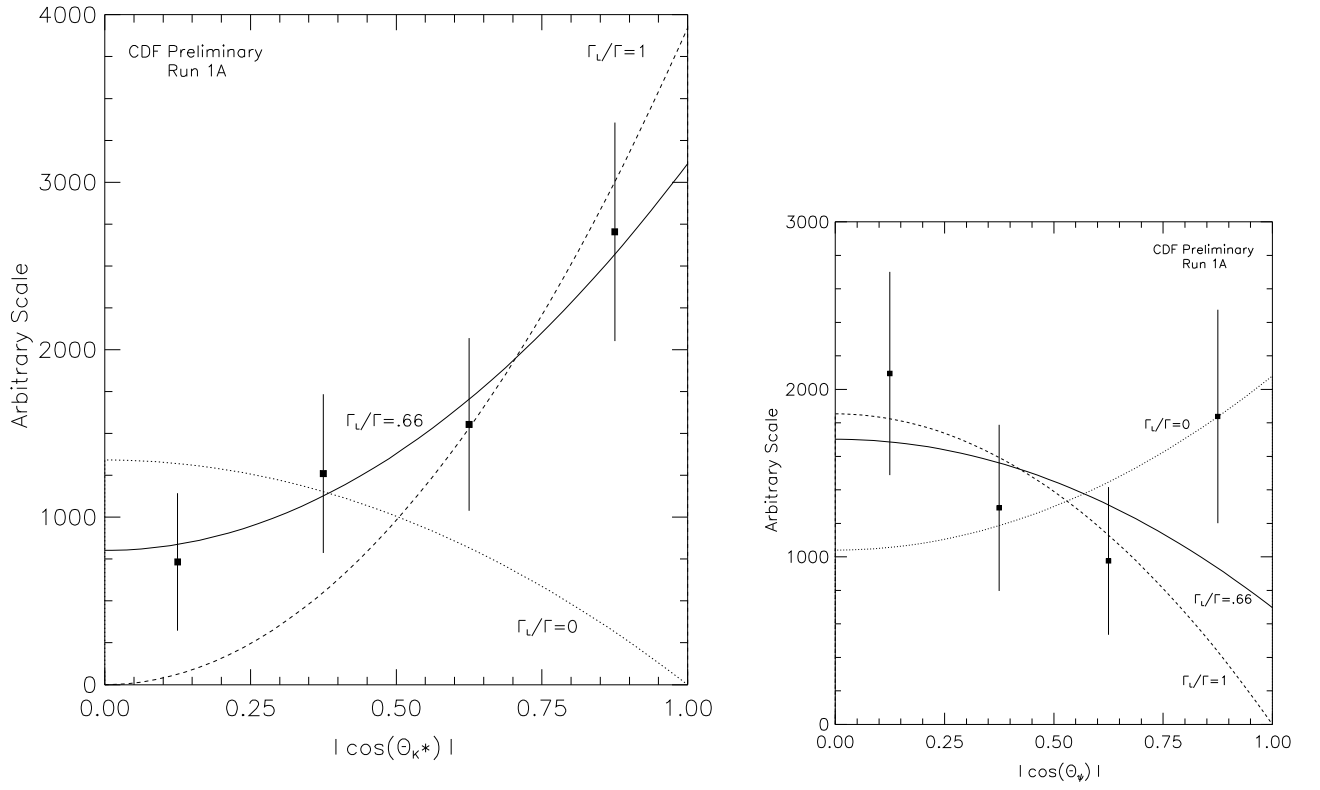


Figure 11: (a) K^{*0} helicity angle distribution. (b) J/ψ helicity angle distribution. The fit value of $\Gamma_L/\Gamma = 0.67$ is shown with the extremes.

AC-coupled SVX detector, we expect to provide more interesting measurements in B physics including:

- Improved measurement of cross section, $b\bar{b}$ correction, and lifetime.
- Search for new states (Λ_b , B_C ...).
- Improve limits on the rare decays $B \rightarrow \mu\mu K$, $B \rightarrow \mu\mu K^*$.
- Observation of time-dependent B mixing.
- Search for exclusive $b \rightarrow u$ decays.
- Search for $B \rightarrow K^*\gamma$.
- Measurements of flavor-tagging efficiencies and dilution factors for CP measurements.

In conclusion, B physics at Fermilab is still in its infancy. The CDF vertex detector expanded the opportunities enormously, and prospects for the future are very exciting.

Acknowledgments

I wish to thank the organizers of the SLAC Summer Institute for their hospitality and the editing staff whose extraordinary patience made it possible to complete this article. I would like to thank the many people who provided me with detailed information about their results.

References

- [1] F. Abe *et al.*, Fermilab-Pub-94/097-E, submitted to Phys. Rev. D.
- [2] S. Abachi *et al.*, Phys. Rev. Lett. **72**, 2138 (1994).
- [3] B. Pietrzyk for the LEP collaborations and the LEP Electroweak Working Group, Laboratoire de Physique des Particules, preprint LAPP-EXP-94.07 (May 1994).
- [4] Here, $P_T = P \sin \theta$, where θ is the polar angle with respect to the proton beam direction. The pseudorapidity, η , is defined as $-\ln \tan \frac{\theta}{2}$.
- [5] F. Abe *et al.*, Nucl. Instrum. Methods Phys. Res., Sect. A **271**, 387 (1988).
- [6] D. Amidei *et al.*, Fermilab-Pub-94/024-E, submitted to Nucl. Instrum. Methods Phys. Res.
- [7] Corrections to the observed jet energy and \cancel{E}_T are described in Ref. 1 and references therein.
- [8] F. Paige and S. D. Protopopescu, BNL Report No. 38034 (1986).
- [9] E. Laenen, J. Smith, and W. L. Van Neerven, Phys. Lett. B **321**, 254 (1994).
- [10] J. Ohnemus *et al.*, Phys. Rev. D **44**, 1403 (1991); S. Frixione, Nucl. Phys. B **410**, 280 (1993).
- [11] P. Avery, K. Read, and G. Trahern, Cornell Internal Note CSN-212, 1985.
- [12] F. A. Berends, W. T. Giele, H. Kuijf, and B. Tausk, Nucl. Phys. B **357**, 32 (1991).
- [13] M. L. Mangano, Nucl. Phys. B **405**, 536 (1993).
- [14] O. Dahl, T. Day, F. Solmitz, and N. Gould, Lawrence Berkeley Laboratory, Physics Division, Group A Programming Note, 126 (1968).
- [15] R. Jesik *et al.*, Fermilab-Pub-94/095-E, submitted to Phys. Rev. Lett.

- [16] M. Schub *et al.*, Fermilab-Pub-95/058-E (1995).
- [17] F. Abe *et al.*, Fermilab-Pub-93/145-E, submitted to Phys. Rev. Lett.
- [18] F. Abe *et al.*, Fermilab-Pub-93/106-E, submitted to Phys Rev. Lett.
- [19] D. Hedin for the D \emptyset Collaboration, in the *Proceedings of the 27th International Conference on High Energy Physics*, Glasgow (1994).
- [20] F. Abe *et al.*, Phys. Rev. Lett. **72**, 3456-3460 (1994).
- [21] F. Abe *et al.*, Fermilab-CONF-95/234-E, submitted to LP95 in Beijing.
- [22] Particle Data Group, K. Hikasa *et al.*, Phys. Rev. D **45**, S1 (1992).
- [23] F. Abe *et al.*, Phys. Rev. Lett. **74**, 4988 (1995).
- [24] F. Abe *et al.*, Fermilab-Pub-95/270-E, submitted to Phys. Rev. Lett.
- [25] M. Alam *et al.*, Phys. Rev. D **50**, 43 (1994).